Oxidation of indium in gold-indium alloys

A. F. Pasquevich
Departamento de Física, Universidad Nacional de La Plata, c.c. 67, 1900 La Plata, Argentina

A. Hoffmann, R. Vianden, and U. Wrede
Institut für Strahlen und Kernphysik der Universität Bonn, D-5300 Bonn, Germany

(Received 27 March 1985; accepted for publication 2 July 1985)

The oxidation in air of *Au*In alloys with low indium content (1 ppm, 0.1 and 1.0 at. %) was investigated with the help of the time-differential perturbed angular correlation technique. From the results it is concluded that the oxidation is external and is independent of solute concentration. While in the concentrated alloys, the oxide formed was In_2O_3, in the cases of the dilute ones, In-O-Au complexes appeared. From the oxidation rate in the temperature range 300–1000 °C values of the frequency factor $A = 0.006(10)$ cm^2/s and the activation energy $Q = 29.0(5)$ kcal/mol for the diffusion of indium in gold were obtained.

I. INTRODUCTION

Although internal oxidation processes in gold-based binary alloys seem to be very unlikely because of the low solubility of oxygen in gold, the existing experimental information is not conclusive.

In studies performed on gold alloys with Ni,[1,2] Cu,[3] and Pd,[4] external oxidation of the solutes was observed. In these cases the solute concentration was greater than 0.5 at. % and, as far as we know, no studies on more dilute alloys have been reported. But there are some studies of the oxidation of impurities in nominally pure gold:

(i) Auger electron spectroscopy has given evidence of surface segregation of trace bulk impurities when gold surfaces are heated in the presence of oxygen.[5,6]

(ii) A conductivity increase of gold samples after annealing in oxidizing atmosphere has been reported in several cases.[7] In this context Svoboda[7] identified the process involved in the improvement of effective purity of gold samples with the internal oxidation of impurities. His interpretation was mainly based on the fact that after subsequent hydrogen annealings the initial impurity content was again observed in the matrix.

One of the aims of the present study was to establish whether an internal oxidation process could take place in very dilute gold alloys. *Au*In alloys were studied by means of the time-differential perturbed angular correlation (TDPAC) technique using ^{111}In atoms as probes. With this technique it is possible to determine the type of the oxide formed and estimate the fraction f of the probe atoms oxidized in the annealing process. This application of the TDPAC technique has been discussed in the literature.[8,9] Unfortunately, this technique is not sensitive to the location of the probe atoms (whether they are on the surface or in the bulk sample). In order to decide whether the oxidation has been external or internal, a comparison of the experimental f values with those calculated assuming each possibility is necessary.

In Sec. II we will present different approaches to the oxidation problem. The experimental procedure and the results will be presented in Secs. III and IV. Discussion and conclusions will be given in Sec. V. Finally, the main conclusions will be summarized in Sec. VI.

II. OXIDATION MODELS

Annealing of binary alloys, based on a noble metal, in the presence of oxygen leads to the growth of solute oxide if the free energy of formation of the oxide is negative. It can be found dissolved in the matrix (internal oxidation) or constituting a surface layer (external oxidation), depending on the oxygen solubility and diffusivity in the alloy as well as on the concentration and diffusivity of the solute.

In the literature,[10] oxidation is discussed assuming that the alloy is a semi-infinite medium. As far as we know, there are no calculations for the internal oxidation of finite sheets. So, we will consider the expressions describing the kinetics of internal oxidation of a semi-infinite medium and discuss its applicability for the case of finite samples.

The internal oxidation occurs by diffusion of oxygen in the base metal. An oxidation front is established at the depth $x = \xi$. As a result, the free-oxygen concentration at depth $x > \xi$ is zero, while the concentration of nonoxidized solute $N_A(x, t)$ is zero for $x > \xi$. According to Wagner's theory[11] the advance of the oxidation front is a parabolic function of time t expressed as

$$\xi^2 = kt, \tag{1}$$

if the oxidation process is controlled by diffusion.

It is possible to establish a relation between the constant k in Eq. (1) and the parameters that rule the oxidation process, that is, with the oxygen concentration in the surface N_0^S, the solute concentration in the alloy $N_A^0 = N_A(x, 0)$, and the diffusivity D_0 and D_A of oxygen and the solute, respectively, in the alloy. In the present case it can be assumed that, due to the extremely low solubility of oxygen in gold,[12] the oxygen concentration in the surface is much smaller than the initial solute concentration. Further, since the small oxygen atom should diffuse interstitially in gold, it can be assumed that its diffusivity is much larger than that of the substitutional solute.

Now, two limiting cases can be distinguished. If the conditions

$$D_A/D_0 \ll N_0^S/N_A^0 \ll 1 \tag{2}$$

are valid, the concentration profiles will be like those drawn in Fig. 1(a) and the oxidation constant will be given by

 0021-8979/85/203200-06$02.40

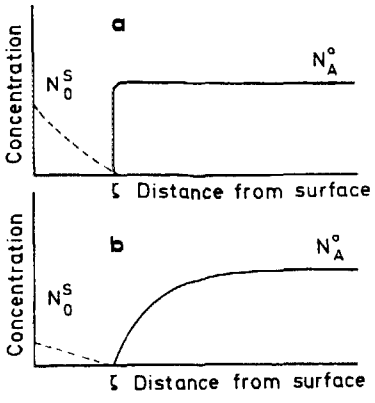

FIG. 1. (a) and (b), concentration profiles under the conditions of Eqs. (2) and (4), respectively. The full lines show the concentration of unoxidized solute and the dashed ones the concentration of free oxygen. N_0^S is the oxygen concentration at the surface. N_A^0 is the solute concentration in the alloy. The oxidation front is located at distance ξ from the surface.

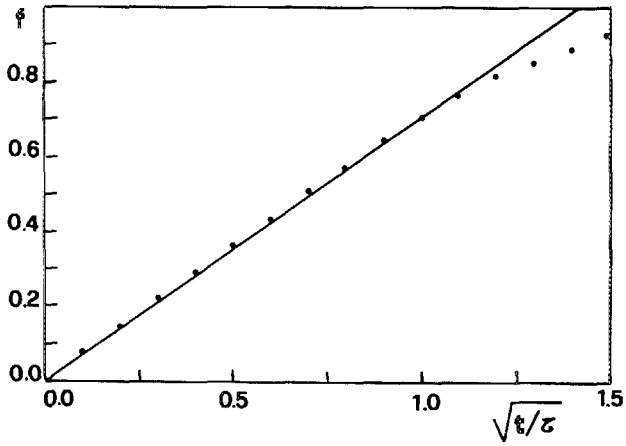

FIG. 3. Fraction of oxidized solute f vs $\sqrt{(t/\tau)}$. τ is the time for a solute oxidation of 70%. The dots were obtained from Eq. (7) with $\beta = \exp(-t/\tau)$. The solid line is a graph of Eq. (8).

$$k = 2 N_0^S D_0 / \nu N_A^0, \tag{3}$$

where ν is the number of oxygen atoms per solute atoms in the oxide.

On the other hand, if the relations

$$N_0^S/N_A^0 \ll D_A/D_0 \ll 1 \tag{4}$$

hold, then the rate of internal oxidation is dependent upon the rate of outward diffusion of the solute atoms and the rate of inward diffusion of oxygen. In this case the concentration profiles are as shown in Fig. 1(b), and the coefficient k is given by

$$k = \pi D_0^2 (N_0^S)^2/\nu^2 (N_A^0)^2 D_A. \tag{5}$$

In the second situation, an enrichment of the solute as oxide in the oxidized zone and a depletion of the same from the unoxidized alloy will result, especially when N_0^S and D_0/D_A are relatively small.

When conditions (2) are satisfied it is possible to use the expression (3) for the case where the oxidation occurs from both faces of a finite sheet of thickness d. The relation between the depth ξ and the fraction f of oxidized atoms is

$$f = 2\xi/d. \tag{6}$$

There is no such obvious relation if conditions (4) are valid. Furthermore, it is not possible to extend expression (5) to the case of interest here, but it seems reasonable that in the finite case also a solute concentration dependence of the oxidation rate can be expected.

Now we will consider the case of external oxidation in the finite sheet geometry. The oxidation will occur by the diffusion of the solute towards the surface. The kinetics of this process will be given by the solution of the diffusion equation with uniform solute distribution and with infinite sinks at the sheets surfaces, as initial and boundary conditions, respectively. The fraction f of solute which has diffused to the surfaces after a time t is[13]

$$f = 1 - (8/\pi^2)\sum_0^\infty [\beta^{(2n+1)2}/(2n+1)^2], \tag{7}$$

where $\beta = \exp(-D_A \pi^2 t/d^2)$.

In Fig. 2 f is plotted versus β. Figure 3 shows the dependence of f on $\sqrt{(t/\tau)}$ and it can be seen that for $f < 0.7$ f is given in a good approximation by

$$f = \sqrt{(t/2\tau)}. \tag{8}$$

Here τ is the time required to oxidize 70% of the solute.

So, both models lead to a parabolic dependence of f on the time of oxidation t. But only the external oxidation model shows that f is independent of the solute concentration.

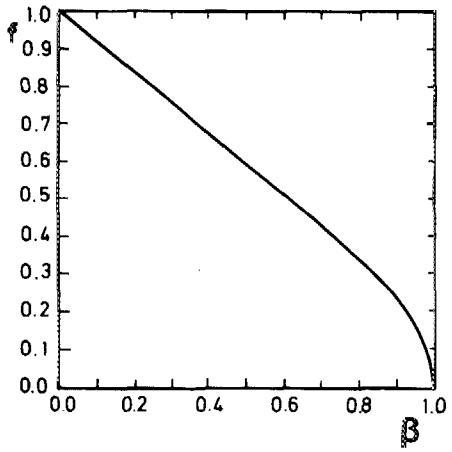

FIG. 2. Fraction of oxidized solute f vs the dimensionless parameter β.

III. EXPERIMENT

The samples were prepared by doping gold and *Au*In foils with ^{111}In. The composition and purity of the specimens studied are shown in Table I. The foils were rolled to adequate thicknesses (5–110 μm) and were then annealed in vacuum (500–700 °C) for 1 h.

Oxidation treatments were carried out by heating the samples in air, the temperature range was 300–1000 °C, and oxidation time was chosen long enough so as to get a sufficient fraction of oxidized solute atoms.

TABLE I. Composition and purity of the samples used.

Specimen type	Gold purity (at. %)	Indium content (at. %)
A	99.90	10^{-4}
B	99.99	10^{-4}
C	99.99	0.1
D	99.99	1.0

The oxidation of the solute atoms was detected by the TDPAC technique. This method is based on the observation of the electric quadrupole interaction (QI) between the electric field gradient tensor (EFG), described by its main component V_{zz} and the asymmetry parameter η, and the nuclear quadrupole moment Q of the intermediate state of a γ-γ cascade in the decay of the radioactive probe atom. Before the oxidation the probe atoms occupy substitutional lattice sites with cubic symmetry and the EFG vanishes. After oxidation a QI due to the existence of EFG's created by the oxygen present in the neighborhood of the probe atoms appears. The characteristics of these QI's were determined by measuring the perturbation of the angular correlation of the 171–245-keV γ-γ cascade emitted in the decay of ^{111}In. The measurements were performed using a standard slow-fast coincidence system with either 3 NaI(Tl) or 4 CsF detectors.[14]

A description of the data analysis can be found in Ref. 9. Experimental anisotropy ratios were evaluated and fitted with theoretical functions of the form $A_2G_2(t)$ folded with the measured time resolution curve.

The assumed perturbation factor was of the form:

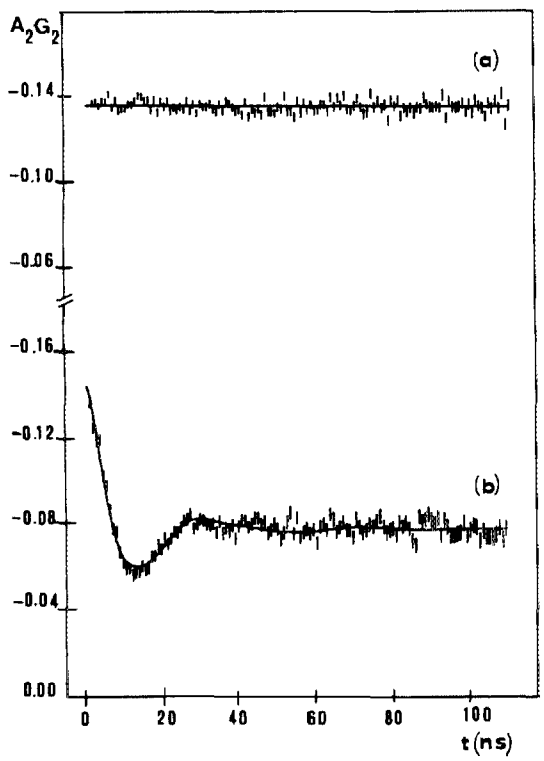

FIG. 4. $A_2G_2(t)$ curves obtained with a type B sample (thickness $d = 29$ μm). (a) Before oxidation. (b) After oxidation in air (75 min, 550 °C).

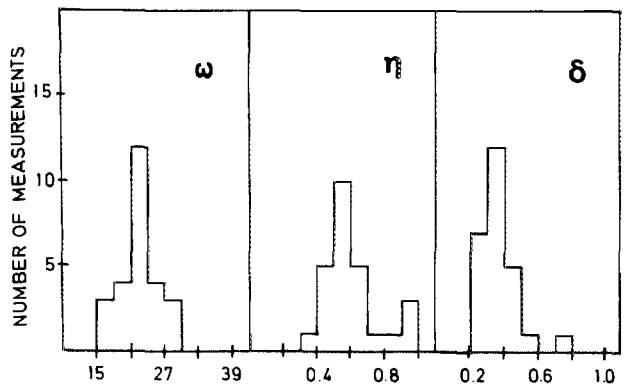

FIG. 5. Histograms of hyperfine interaction parameters measured in samples of types A and B. ω_Q values are in Mrad/s. η and δ are dimensionless parameters.

$$G_2(t) = f_0 + \sum_i f_i \sum_{n=0}^{3} s_{ni} \exp(-\delta_i \omega_{ni} t) \cos(\omega_{ni} t), \quad (9)$$

where f_i are the relative fractions of probe atoms that experience a given perturbation and f_0 corresponds to unperturbed probes. The frequencies ω_n are related to the quadrupole interaction frequency $\omega_Q (= eQV_{zz}\pi/20\,\mathrm{h})$ by the relation $\omega_n = F_n(\eta)\omega_Q$. The coefficients F_n and s_n are known functions[15] of η. The exponential function accounts for a Lorentzian frequency distribution of relative width δ around ω_n.

IV. RESULTS

In Fig. 4 TDPAC spectra for a very dilute sample taken before and after oxidation are shown. Figure 4(a) corresponds to 100% of the In-probe atoms on unperturbed substitutional lattice sites. The electric quadrupole interaction observed in all the very dilute samples (types A and B) after oxidation has the same characteristic: a broad distribution of electric field gradients at the probe sites [Fig. 4(b)]. The values of the parameters ω, η, and δ characterizing the hyperfine interaction of the oxidized probes are not sensitive to the temperature and duration of the oxidation process. There is some spread in those values as shown in Fig. 5, where their distribution over 26 independent measurements is presented.

The effect of annealing a previously oxidized very dilute sample in vacuum ($p < 10^{-5}$ mbar) can be seen by comparing the TDPAC spectra shown in Fig. 6 and one finds that more than 90% of the probe atoms are again in unperturbed lattice sites.

The oxidation of the alloys with larger solute concentrations (types C and D) leads to TDPAC spectra that are definitively different. A typical one is displayed in Fig. 7. In this kind of spectra the two following static interactions

(1) $\omega_Q = 18.1(1.0)$ Mrad/s $\quad \eta = 0.74(0.02)$
$\quad \delta = 0.05(0.01)$

(2) $\omega_Q = 24.7(1.0)$ Mrad/s $\quad \eta = 0.25(0.05)$
$\quad \delta = 0.01(0.01)$

are observed with an amplitude ratio of 3 : 1.

In some of the samples with indium concentration of

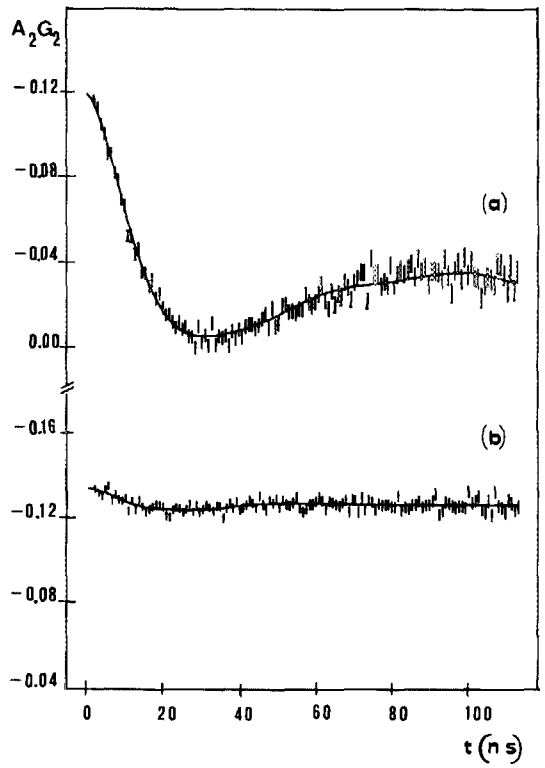

FIG. 6. $A_2G_2(t)$ curves obtained with a type A sample ($d = 32\,\mu$m). (a) After oxidation in air (30 min, 750 °C). (b) After subsequent annealing in vacuum (90 min, 950 °C, 10^{-5} mbar).

1 at. % (type D) the presence of a time-dependent interaction was observed. In general this effect was not very important and the values of the oxidized fractions remain practically the same when it was taken into consideration in the fitting procedure.

In all the measurements performed on samples with 0.1-at. % In content a third static component appeared and was characterized by the following parameters:

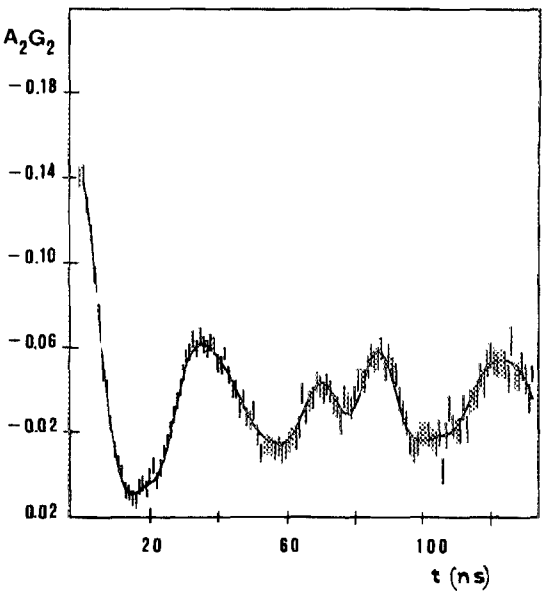

FIG. 7. $A_2G_2(t)$ curve obtained with a type D sample ($d = 70\,\mu$m) after oxidation in air (4 min, 1000 °C).

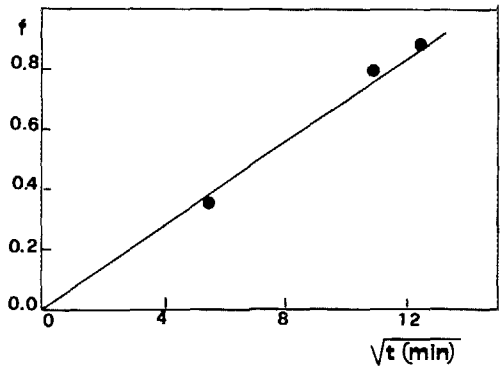

FIG. 8. Fraction of oxidized probes vs the square root of time of oxidation for a type A specimen. ($T = 550$ °C). The straight line corresponds to a parabolic rate of oxidation.

$\omega_Q = 35.5(1.0)$ Mrad/s $\quad \eta = 0.39(0.05) \quad \delta = 0.11(0.02)$.

In Fig. 8 the fraction of oxidized probe atoms versus the square root of the time of oxidation for a very dilute sample has been plotted. It can be seen that the fraction f shows a nearly parabolic time dependence. In order to investigate whether the process corresponds to an internal oxidation it is convenient to analyze the following data combination

$$z = \ln (f^2 d^2 / t). \tag{10}$$

If the oxidation is internal, z [then proportional to $\ln(4k)$, as can be seen from Eqs. (1) and (6)] should show a linear dependence with the reciprocal oxidation temperature:

$$z = [a(10^3)/T] + b. \tag{11}$$

In Fig. 9 the values of z are plotted as a function of the

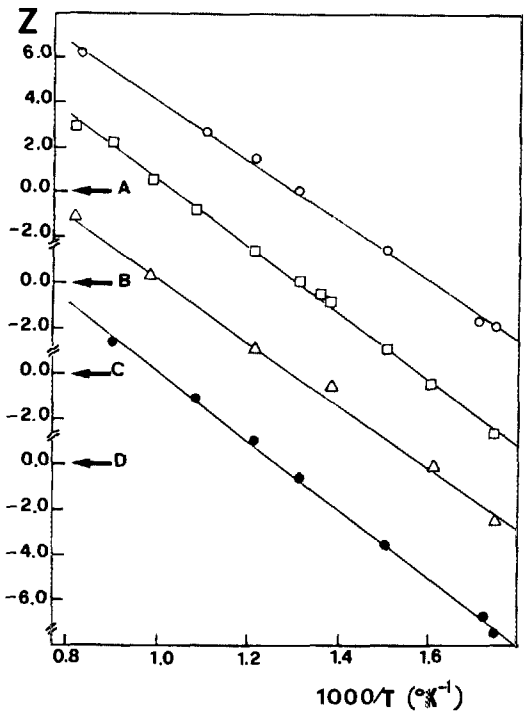

FIG. 9. z values vs $10^3/T$. z was calculated with expression (10), using the thickness d in μm and t in minutes. Data for specimens of type A (○), B (□), C (△), and D (●) are shown with the corresponding scales shifts. The arrows indicate the different zero points.

TABLE II. Results of least-square fits for constants a and b in Eq. (11).

Specimen type	$a(K^{-1})$	b
A	13.3(0.2)	17.5(0.9)
B	14.6(0.3)	19.1(1.1)
C	13.9(0.5)	18.1(1.5)
D	15.2(0.3)	19.3(1.0)

reciprocal oxidation temperature for the whole set of analyzed samples. In those cases in which more than one interaction was present, f was taken as the sum of the individual fractions. The straight lines are the result of least squares fits of the expression (11) to the z values. In Table II results for constants a and b are shown. a should be related to the activation energy for internal oxidation and b should be a linear function of $\ln(\nu N_A)$, as can be seen from Eq. (3).

In order to consider the possibility of external oxidation we can treat the data according to Eq. (7) or the graph plotted in Fig. 2. Thus, it is possible to associate one value of the diffusivity D to each set (f, d, T, t). The values obtained for $\ln D$ are plotted in Fig. 10 as a function of reciprocal temperature. The straight line results from a least squares fit of the expression $D = Ae^{-Q/RT}$ to the data. For the parameters the following values are obtained: $A = 0.006(10)$ cm^2/s and $Q = 29.0(5)$ kcal/mol.

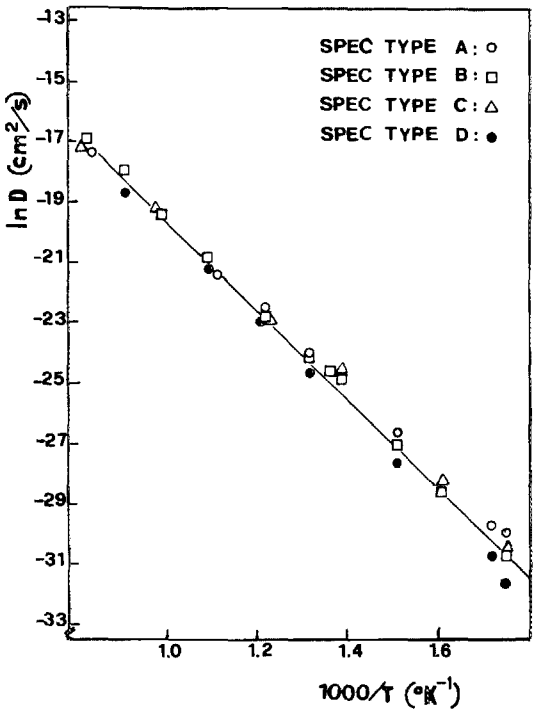

FIG. 10. Arrhenius plot of the diffusivity D vs $10^3/T$.

V. DISCUSSION AND CONCLUSIONS

Although the measured values of the frequency for the samples with low indium content are, in average, higher than those reported in the oxidation of the system *Ag*In with comparable indium concentration,[8,16] it seems reasonable to assume that the interaction arises from the formation of several configurations of indium-oxygen complexes. These complexes are similar to those already observed in silver matrices, which also dissociated upon annealing in vacuum at high temperature. The multiplicity of configurations is evidenced by the broadly distributed interaction. The difference between the frequencies associated with complexes in silver and gold can be related to the influence of the matrix and also to the fact, as we will show below, that in the gold matrix the Au-O-In complexes form in the sample surface while in the Ag case the Ag-O-In complexes are in bulk.

The results obtained for the samples with higher indium content correspond to the formation of indium sesquioxide (In_2O_3). Indeed, the hyperfine parameters we measured with samples of high indium content are characteristic for this oxide.[9,17] The fact that we observe only a weak time-dependent interaction can be related to the influence of the metallic matrix on the oxide conductivity.[18]

The third static component present in samples of 0.1-at. % indium content has not been observed previously in TDPAC experiments of oxidation involving indium. Its amplitude corresponds approximately to 25% of the probe atoms and is independent of the fraction of atoms that experience the interactions associated with In_2O_3. The involved fraction has been added to the fraction of oxidized probes. The validity of this procedure will be justified below. As can be seen from Fig. 9 and Table II the values of the slope are nearly independent of solute concentration. Therefore, we can exclude different oxidation processes for samples with low and high In content.

The result of Svoboda concerning the recovery of oxidized samples upon annealing in reducing atmosphere has been confirmed by our observation. Annealing in vacuum leads to the appearence of an important fraction of probe atoms dissolved in the matrix as can be seen from the nearly unperturbed result shown in Fig. 6(b). However, this fact is not sufficient to conclude that the oxidation was internal. Furthermore, the present results indicate the opposite conclusion. The values of the parameter b displayed in Table II are independent of solute concentration N_A and this fact is not consistent with what is expected for an internal oxidation process since b should then depend on the product νN_A. Although the mean stoichiometry of the complexes formed in the very dilute alloys is unknown, it is improbable that the variation of ν compensates that of N_A. Thus, we can conclude that our results are described better by an external oxidation process.

The deoxidation experiment is compatible with an external oxidation process since both temperature and duration of the annealing, being comparable to those of the experiment of Svoboda, allow the dissociation of external oxide and the inward diffusion of the solute.

We now will discuss the third static component that appears only in the samples with 0.1-at. % indium. The connection of this interaction with a surface effect in the film of In_2O_3 cannot explain that the amplitude of this component is nearly independent of the thickness of the foils. This behavior can be explained if the existence of some impurity in the samples is assumed. The concentration of this impurity must be so low that it is only relevant in the case of samples with medium In content. This impurity must diffuse faster than

indium in order to explain the observation that the amplitude of the third component is independent of the oxidation times used in these experiments. The interaction is then caused by the trapping of this impurity in the In_2O_3 layer. In the case of the very dilute samples, the In concentration is not high enough to build such a trapping layer. The impurity involved could be carbon, possibly introduced into the sample during preparation. These assumptions will be checked in further experiments.

If the argumentation above is valid, the third fraction is due to the oxidation of the probe atoms. If not, the consistency of the diffusivity results obtained with samples with 0.1-at. % In content with those obtained with the other samples (see Fig. 10) shows that this third fraction arises from an oxidationlike reaction, in the sense of an infinite sink without changing the rate of the process. In both cases it is justified to add the third fraction to the oxidized probes one.

The model assumed in order to explain the rate of oxidation does not take into account the influence of the oxide layer but the low In concentrations involved in our experiments justify this approximation. Besides, it is assumed in the model that the solute has the same mobility throughout the whole material, though a more realistic approach should take into account that the solute diffuses through the bulk and grain boundaries while moving outward. Therefore, without a knowledge of the grain size it is impossible to discuss the coupling between bulk and grain boundary diffusion that results in the measured value of the diffusivity.

Finally, it is shown in this work that it is possible to apply the TDPAC technique to determine diffusivities of radioactive impurities in metallic matrices by measuring the increase of the oxide signal as it has been done with Auger electron spectroscopy in permeation studies.[19]

VI. SUMMARY

The oxidation of the solute In in gold-based binary alloys is external.

The formed indium oxides have structures similar to those found in the oxidation of silver-indium alloys. The difference in the quadrupole interaction frequencies associated with equivalent In-O complexes may be due to the fact that the oxide is external in this case and to the influence of the different base metal.

Finally, values for the diffusivity of indium in gold are obtained in a broad temperature range, showing that the TDPAC technique can be used to get information about diffusion processes.

ACKNOWLEDGMENTS

This work was partially supported by the Deutsche Forschungsgemeinschaft and the Bundesminister für Forschung und Technologie. One of us (A.F.P.) acknowledges the support of the Comisión de Investigaciones Científicas de la Provincia de Buenos Aires (CICPBA), Argentine and Deutscher Akademischer Austauschdienst (DAAD), West Germany.

[1]M. R. Pinnel, H. G. Tomkins, and D. E. Heath, J. Electrochem. Soc. **126**, 1274 (1979).
[2]C. Wagner and K. Grünewald, Z. Phys. Chem. B **40**, 455 (1932).
[3]M. R. Pinnel, H. G. Tomkins, and D. E. Heath, J. Electrochem. Soc. **126**, 1798 (1979).
[4]G. Maire, L. Hilaire, P. Legare, F. G. Gault, and A. O'Cinneide, J. Catalysis **44**, 293 (1976).
[5]M. A. Chesters and G. A. Somorjai, Surf. Sci. **52**, 21 (1972).
[6]M. E. Schrader, Surf. Sci. **78**, L227 (1978).
[7]P.Svoboda, J. Phys. F **8**, 1757 (1978); and references cited therein.
[8]A. F. Pasquevich, F. H. Sánchez, A. G. Bibiloni, J. Desimoni, and A. López García, Phys. Rev. B **27**, 963 (1983).
[9]J. Desimoni, A. G. Bibiloni, L. Mendoza-Zélis, A. F. Pasquevich, F. H. Sánchez, and A. López García, Phys. Rev. B **28**, 5739 (1983).
[10]G. R. Wallwork, Rep. Prog. Phys. **39**, 401 (1976).
[11]C. Wagner, J. Electrochem. Soc. **63**, 777 (1959).
[12]W. Eichenauer and D. Liebscher, Z. Naturf. A **17**, 355 (1962).
[13]W. Jost, *Diffusion in Solids, Liquids, Gases* (Academic, New York, 1960).
[14]A. R. Arends, C. Hohenemser, F. Pleiter, H. De Waard, L. Chow, and R. M. Suter, Hyperfine Interactions **8**, 191 (1980).
[15]L. A. Mendoza-Zélis, A. G. Bibiloni, M. C. Caracoche, A. López García, J. A. Martínez, R. C. Mercader, and A. F. Pasquevich, Hyperfine Interactions **3**, 315 (1977).
[16]P. Wodniecki and B. Wodniecka, Hyperfine Interactions **12**, 95 (1982).
[17]M. Uhrmacher and W. Bolse, Hyperfine Interactions **15/ 16**, 455 (1983).
[18]A. G. Bibiloni, J. Desimoni, C. P. Massolo, L. Mendoza-Zélis, A. F. Pasquevich, F. H. Sánchez, and A. López-García, Phys. Rev. B **29**, 1109 (1984).
[19]J. C. M. Hwang, J. D. Pan, and R. W. Balluffi, J. Appl. Phys. **50**, 1349 (1979).